



Protective effects of palbociclib on colitis-associated colorectal cancer

Li Yang^{1,2#}, Jiani Gao^{3#}, Yuqin Zhang^{2,4#}, Eduardo A. Perez⁵, Yuchen Wu^{1,2}, Tianan Guo^{1,2}, Cong Li^{1,2}, Hao Wang^{3,6}, Ye Xu^{1,2}

¹Department of Colorectal Surgery, Fudan University Shanghai Cancer Center, Shanghai, China; ²Department of Oncology, Shanghai Medical College, Fudan University, Shanghai, China; ³Department of Thoracic Surgery, Shanghai Pulmonary Hospital, Tongji University School of Medicine, Shanghai, China; ⁴Department of Oncology Surgery, Fudan University Shanghai Cancer Center, Minhang District, Shanghai, China; ⁵Daughtry Family Department of Surgery, University of Miami Miller School of Medicine, Miami, FL, USA; ⁶Endoscopy Center, Shanghai Pulmonary Hospital, Tongji University School of Medicine, Shanghai, China

Contributions: (I) Conception and design: L Yang, Y Xu, H Wang; (II) Administrative support: Y Xu, H Wang; (III) Provision of study materials or patients: L Yang, J Gao; (IV) Collection and assembly of data: J Gao, Y Zhang, T Guo, C Li; (V) Data analysis and interpretation: J Gao, Y Zhang, Y Wu; (VI) Manuscript writing: All authors; (VII) Final approval of manuscript: All authors.

[#]These authors contributed equally to this work.

Correspondence to: Ye Xu, MD, PhD. Department of Colorectal Surgery, Fudan University Shanghai Cancer Center, 270 Dong'an Road, Shanghai 200032, China; Department of Oncology, Shanghai Medical College, Fudan University, Shanghai, China. Email: yexu@shmu.edu.cn; Hao Wang, MD. Department of Thoracic Surgery, Shanghai Pulmonary Hospital, Tongji University School of Medicine, 507 Zhengmin Road, Shanghai 200092, China; Endoscopy Center, Shanghai Pulmonary Hospital, Tongji University School of Medicine, Shanghai, China. Email: shfknj@163.com.

Background: Chronic or recurrent inflammatory injury to the intestinal mucosa is closely related to inflammation-related colorectal cancer (CRC). This study aimed to examine the protective effects of palbociclib, a stimulator of interferon genes (STING) antagonist, on colitis-related colorectal carcinogenesis.

Methods: Bioinformatic analyses, including Gene Ontology (GO) enrichment, gene set enrichment analysis (GSEA), and network analysis, were conducted. Male C57BL/6 mice were administered azoxymethane (AOM) and dextran sulfate sodium (DSS), followed by treatment with palbociclib for 6 weeks. The general conditions of mice were observed and recorded. The colon histopathology was assessed based on hematoxylin and eosin (H&E) staining results. Relative messenger RNA (mRNA) expression levels of interferon b1 (*Ifnb1*), interleukin 6 (*Il6*), and interleukin 1b (*Il1b*) in colon were estimated based on quantitative real-time reverse transcription polymerase chain reaction (qRT-PCR) analysis.

Results: The STING signaling pathway was significantly upregulated in stages III and IV of CRC in The Cancer Genome Atlas (TCGA)-CRC cohort. After treatment with AOM/DSS, the weight of mice decreased significantly, whereas administration of palbociclib partially reversed this trend. The mouse colon treated with AOM/DSS showed significant pathological damages, disorderly epithelial cell structure, atypical hyperplasia, and infiltration of several inflammatory cell types; however, the colon damage was remarkably reduced upon treatment with palbociclib. It was also found that palbociclib almost abolished the increase in the downstream effectors of STING-mediated transcription in the colon tissue treated with AOM/DSS, as evidenced by the transcription levels of *Ifnb1*, *Il6*, and *Il1b*.

Conclusions: These findings indicate that the STING pathway is closely associated with CRC. Palbociclib significantly alleviates tumor development in AOM/DSS-induced colitis-associated CRC.

Keywords: Palbociclib; colitis-associated colorectal cancer (CAC); stimulator of interferon genes (STING); agonists; cyclin-dependent kinases (CDKs)

Submitted Oct 20, 2023. Accepted for publication Dec 13, 2023. Published online Dec 27, 2023.

doi: 10.21037/jgo-23-860

View this article at: <https://dx.doi.org/10.21037/jgo-23-860>

Introduction

Colorectal cancer (CRC) poses a significant public health challenge. In both males and females, CRC ranks second in mortality and third in incidence worldwide (1). Inflammatory bowel disease (IBD), which includes ulcerative colitis and Crohn's disease, is a chronic intestinal inflammatory disease prone to relapse. These patients are at substantially high risk of CRC, which increases with the duration of IBD (2).

Colitis-associated CRC (CAC) is a particularly feared complication associated with IBD, as these patients are frequently diagnosed with locally advanced or metastatic disease at an advanced stage. Unlike more common sporadic CRC arising from polyps, identification of pre-cancerous dysplastic lesions or early CAC in patients with IBD is challenging. The flat appearance makes it difficult to determine the total extent of the pre-cancerous area and is hard to remove it by endoscopy. CAC confers a poorer prognosis relative to sporadic CRC as it is relatively poorly differentiated and occurs at multiple sites (3).

Given the microenvironment of CRC and colitis-associated dysplasia, it is speculated that the immune and inflammatory responses of the host play a crucial role in CAC pathogenesis. The continuous production of chemokines and cytokines from recurrent chronic inflammation leads to persistent migration, proliferation, repair, and damage of intestinal epithelial cells, causing progressive changes in the inflamed colonic mucosa towards a state of tumor-associated molecular signals. Furthermore, an exome-wide analysis revealed that CAC possesses a unique mutational spectrum associated with the dysregulation of inflammatory mediators

related to IBD as compared to sporadic CRC (4).

The stimulator of interferon genes (STING) protein is an important sensor which triggers the production of pro-inflammatory cytokines and type I interferon following activation by cytosolic double stranded DNA (dsDNA) or by bacterially-derived cyclic dinucleotides (cDNs). The cGAS-STING signaling pathway is crucial in maintaining intestinal mucosal homeostasis, but its excessive activation contributes to intestinal inflammation, thus leading to the progression of IBD (5). Furthermore, cGAS-deficient mice exhibit attenuated intestinal inflammation relative to STING-deficient mice, suggesting that STING plays a crucial role in IBD (6). H-151 is one of the most potent inhibitors of STING and a prior study showed that H-151 protects against dextran sulfate sodium (DSS)-induced colitis by reducing inflammation (7). Reports on STING inhibitors are still in the preclinical stages.

Our data from previous studies have shown that through high-throughput screening, palbociclib, a clinically used inhibitor of 4/6 cyclin-dependent kinases (CDKs), is a new inhibitor of STING, which can directly bind to STING and specifically inhibit STING downstream pathways, including type I interferon, inflammatory factors, and autophagy. The inhibitory effect of palbociclib on STING in mice and humans was particularly important. Mechanistically, palbociclib targets STING's Y167 site by preventing STING dimerization; the binding ability of cDNs, the transport of endoplasmic reticulum-Golgi intermediate compartment (ERGIC), and the activation of downstream pathways were further affected. In addition, palbociclib can also block the formation of STING-TBK1 complex through the G166 site, thus inhibiting its activation. Further, we identified that palbociclib could reduce inflammatory responses through inhibiting the STING pathway, thereby protecting against DSS-induced colitis (8).

In this study, we analyzed a public database to examine the relationship between the STING pathway and CRC, and aimed to elucidate the role of palbociclib in inflammation-related CRC and inflammation-cancer transformation. We present this article in accordance with the ARRIVE reporting checklist (available at <https://jgo.amegroups.com/article/view/10.21037/jgo-23-860/rc>).

Methods

Bioinformatic analysis

First, we performed a bioinformatics analysis of The Cancer

Highlight box

Key findings

- The stimulator of interferon genes (STING) pathway was closely associated with colorectal cancer (CRC). Palbociclib significantly alleviated tumor development in colitis-associated CRC (CAC).

What is known and what is new?

- Palbociclib was identified as a potent inhibitor of the STING pathway with protective effects against colitis in our previous study.
- The effect of palbociclib in azoxymethane (AOM)/dextran sulfate sodium (DSS)-induced CAC was found in this study.

What is the implication, and what should change now?

- Palbociclib likely suppresses colon carcinogenesis through the attenuation of inflammation of the colon mucosa. More studies are needed to identify the mechanisms underlying palbociclib's protective effects.

Genome Atlas (TCGA) dataset, which is a cancer genomics program, molecularly characterized over 20,000 primary cancer and matched normal samples spanning 33 cancer types (<https://portal.gdc.cancer.gov/>). Level 3 RNA-seq V2 data sets of TCGA-CRC were obtained, along with the corresponding clinicopathological characteristics from the public database. We obtained a total of 512 CRC patients from TCGA, excluding 14 patients whose tumor stage was not known, finally 498 patients were included in the study. The patient characteristics in TCGA are shown in the *Table 1*. Based on the tumor grade, patients were divided into high- and low-grade groups (I and II were defined as low-grade and III and IV as high-grade). Subsequently, differentially expressed genes (DEGs) across these groups were analyzed, yielding 225 and 93 up- and down-regulated genes, respectively (\log_2 |fold change| ≥ 1.5 and adjusted P value < 0.05 based on edgeR). Gene Ontology (GO) enrichment analysis was performed (based on the web tool, g: profiler) for DEGs (using hypergeometric test, $P < 0.05$). Gene set enrichment analysis (GSEA) was performed, and the gene set involved in the STING pathway was considered as enriched if the normalized enrichment score (NES) > 1 , P value < 0.05 , and false discovery rate (FDR) < 0.25 . The study was conducted in accordance with the Declaration of Helsinki (as revised in 2013).

Animals and groups

C57BL/6 mice were purchased from Shanghai Laboratory Animal Center, CAS, China. Male mice (aged 8–10 weeks) were fed standard laboratory chow and allowed ad libitum access to water. Mice were housed in specific-pathogen-free (SPF) conditions at Tongji University, China. Mice were housed in a double barrier unit within individual micro-isolator cages (Techniplast, Varese, Italy) with HEPA filter lids in a room maintained at 22 ± 1 °C with 65–75% humidity and a 12-h light/dark cycle. Animals were fed for 7 days, and 20 mice were randomly and equally divided into four groups—group 1: control group; group 2: model group [azoxymethane (AOM)/DSS group]; group 3: palbociclib treatment group (AOM/DSS + palbociclib group); group 4: H-151 treatment group (AOM/DSS + H-151 group). No significant differences in age, body weight, water intake, and defecation across groups were observed. A total of five mice per group were used for biological replicates. All animal experiments were performed under a project license (No. K23-048Y) granted by the Ethics Committees of Shanghai

Pulmonary Hospital, in compliance with the institutional guidelines for the care and use of animals. A protocol was prepared before the study without registration.

CAC mouse model

To date, significant advances have been made from studying murine models of CAC. The AOM/DSS model is a powerful, reproducible, and relatively inexpensive initiation-promotion model that utilizes chemical induction of DNA damage followed by repeated cycles of colitis that mimic human colitis-induced CRC. The AOM/DSS model has been widely used in research related to CAC with the advantages of relatively short timeline and accurate modeling of CAC (9,10). Except for the control group, AOM/DSS was used for the induction of mice in all groups to establish a CAC model with reference to previous research methods (11). The mice in group 1 were administered normal drinking water and saline. The mice in groups 2 to 4 were injected intraperitoneally with a single dose of 10 mg/kg AOM and then orally administered 2.5% DSS drinking water for 7 days during weeks 1, 3, and 5. The mice in groups 3 and 4 were also administered palbociclib or H-151 (10 mg/kg/day, ip), concomitant with DSS treatment.

General conditions and disease activity index in each group

The mice were monitored daily for changes in body weight, diarrhea, fecal consistency, and intestinal bleeding. After 6 weeks, the mice were euthanized by cervical dislocation, and the whole colon tissue was excised. After dissection, changes in the morphology and structure of the colon were observed, and the degree and extent of colon congestion, ulcers, erosions, and tumors were observed.

Histological analysis

Colon samples (3–4 cm from the cecum) were fixed in 10% neutral buffered formalin, embedded in paraffin, cut into 5 μ m sections, and stained with hematoxylin and eosin (H&E). The extent of colon tissue damage was assessed by Chiu's pathological scoring standard. A total of 5 sections of the same tissue sample were scored. According to the severity, the mucosal injury score ranged from 1 to 6, and the grade was between 0 and 5. Higher scores indicated more severe intestinal mucosal damage in mice.

Table 1 The characteristic details of patients in TCGA database

Category	Overall (N=512), n (%)
KRAS	
No	26 (5.1)
Not reported	461 (90.0)
Yes	25 (4.9)
Lymphatic invasion	
No	282 (55.1)
Not reported	50 (9.8)
Yes	180 (35.2)
Race	
American Indian or Alaska native	2 (0.4)
Asian	11 (2.1)
Black or African American	65 (12.7)
Not reported	193 (37.7)
White	241 (47.1)
Microsatellite instability	
No	88 (17.2)
Not reported	409 (79.9)
Yes	15 (2.9)
Pathologic M	
M0	370 (72.3)
M1	60 (11.7)
M1a	9 (1.8)
M1b	3 (0.6)
Mx	60 (11.7)
Not reported	10 (2.0)
Pathologic N	
N0	305 (59.6)
N1	80 (15.6)
N1a	16 (3.1)
N1b	16 (3.1)
N1c	2 (0.4)
N2	69 (13.5)
N2a	8 (1.6)
N2b	14 (2.7)
Not reported	2 (0.4)

Table 1 (continued)**Table 1** (continued)

Category	Overall (N=512), n (%)
Pathologic T	
Not reported	2 (0.4)
T1	11 (2.1)
T2	85 (16.6)
T3	349 (68.2)
T4	34 (6.6)
T4a	19 (3.7)
T4b	11 (2.1)
Tis	1 (0.2)
Status	
Alive	395 (77.1)
Dead	115 (22.5)
Not reported	2 (0.4)
Stage	
Not reported	14 (2.7)
Stage I	81 (15.8)
Stage Ia	1 (0.2)
Stage II	41 (8.0)
Stage IIa	151 (29.5)
Stage IIb	12 (2.3)
Stage IIc	1 (0.2)
Stage III	22 (4.3)
Stage IIIa	8 (1.6)
Stage IIIb	64 (12.5)
Stage IIIc	45 (8.8)
Stage IV	52 (10.2)
Stage IVa	18 (3.5)
Stage IVb	2 (0.4)

TCGA, The Cancer Genome Atlas.

RNA extraction and quantitative real-time reverse transcription polymerase chain reaction (qRT-PCR) analysis

Total RNA was isolated from the scraped colon mucosa of experimental mice using the Trizol reagent (15596018; Invitrogen, Waltham, MA, USA) following the

Table 2 The primer sequences of the genes

Gene	Primer sequences
<i>Ifnb1</i>	F: CAGCTCCAAGAAAGGACGAAC
	R: GGCAGTGTAAGTCTTCTGCAT
<i>Il1b</i>	F: GCAACTGTTCTGAACTCAACT
	R: ATCTTTTGGGGTCCGTCAACT
<i>Il6</i>	F: CCAAGAGGTGAGTGCTTCCC
	R: CTGTTGTTGAGACTCTCTCCCT
<i>Gapdh</i>	F: AGGTCGGTGTGAACGGATTTG
	R: TGTAGACCATGTAGTTGAGGTCA

manufacturer's instructions. The total RNA quantity was determined by measuring the optical density at 260 nm using a spectrophotometer. The quality of the RNA samples was evaluated using the RNA 6000 Nano LabChip Kit on an Agilent 2100 Bioanalyzer from Agilent Technologies. All samples met the quality requirement, with a RNA integrity number (RIN) greater than 7. In each sample, a total of 720 ng of RNA was reverse-transcribed into single-stranded complementary DNA (cDNA) using PrimeScript™ II Reverse Transcriptase (FSQ-1012690; Takara, Shiga, Japan). The cDNA was amplified using LookOut Mycoplasma PCR Detection Kit (MP0035; Sigma-Aldrich, St. Louis, MO, USA). The amplification was detected in real-time on the QuantStudio7 Real-Time PCR System (Applied Biosystems, Waltham, MA, USA). The sequences for these primers are listed in *Table 2*. The levels of interferon b1 (*Ifnb1*), interleukin 6 (*Il6*), and interleukin 1b (*Il1b*) expression were normalized to that of glyceraldehyde 3 phosphate dehydrogenase (*Gapdh*).

Statistical analysis

All data were expressed as mean \pm standard error of the mean (SEM) of the average of biological replicates from the indicated number of independent experiments. The gene expression levels were estimated using the comparative ΔC_t method of relative quantification based on qRT-PCR (12). A 2-tailed Student's *t*-test, Mann-Whitney *U*-test, one-way analysis of variance (ANOVA) followed by Dunnett's post hoc test, or 2-way ANOVA followed by Tukey's post hoc test were used accordingly. All the statistical analyses were performed using GraphPad Prism 8 (GraphPad Software, San Diego, CA, USA). Differences with $P < 0.05$ were

considered statistically significant.

Results

Bioinformatic analysis

We investigated 498 CRC samples from the TCGA database, and 318 DEGs (225 and 93 up- and down-regulated genes) were detected through different analyses (see materials and methods). Functional enrichment analysis was conducted to explore the biological importance of those DEGs.

According to the GO annotation results of DEGs, they were enriched in immune-related signaling pathways, including CXCR chemokine receptor binding, chemokine activity, immunoglobulin receptor binding, and humoral immune responses. This suggests the role of immunity in CRC (*Figure 1A, 1B*). According to the results of GSEA, the STING signaling pathway was significantly upregulated in the high-grade group relative to the low-grade group, suggesting its crucial role in the malignant progression of CRC (*Figure 1C*).

The general conditions and histomorphological changes of mice in each group

We set up a DSS/AOM-induced CAC model in mice and examined the effect of palbociclib on the progression of disease (*Figure 2*). As compared to the control group, the body weights of mice in the three groups induced using AOM/DSS decreased significantly ($P < 0.05$). Weight loss was alleviated following treatment with palbociclib or H-151 but the difference was not statistically significant (*Figure 3*).

Histomorphological examination of colon tissue of mice in each group, suggested that the structure of each layer in the control group was clear without obvious abnormalities. The epithelial cells were closely arranged, and there was no remarkable damage to the mucosa and glands (*Figure 4A*). In comparison with the control group, the colonic mucosa of mice in group 2 was damaged. Severe epithelial cell structure disorder, differential morphology, nuclear atypia, high nuclear-cytoplasmic ratio, the disappearance of a large number of glands, atypical hyperplasia, and increased inflammatory cell infiltration level were observed (*Figure 4B*). Relative to group 2, treatment with palbociclib or H-151 showed the following changes: the formation of colonic epithelial tissue tumors decreased, and the colonic mucosal damage, structural disorder, dysplasia, and inflammatory

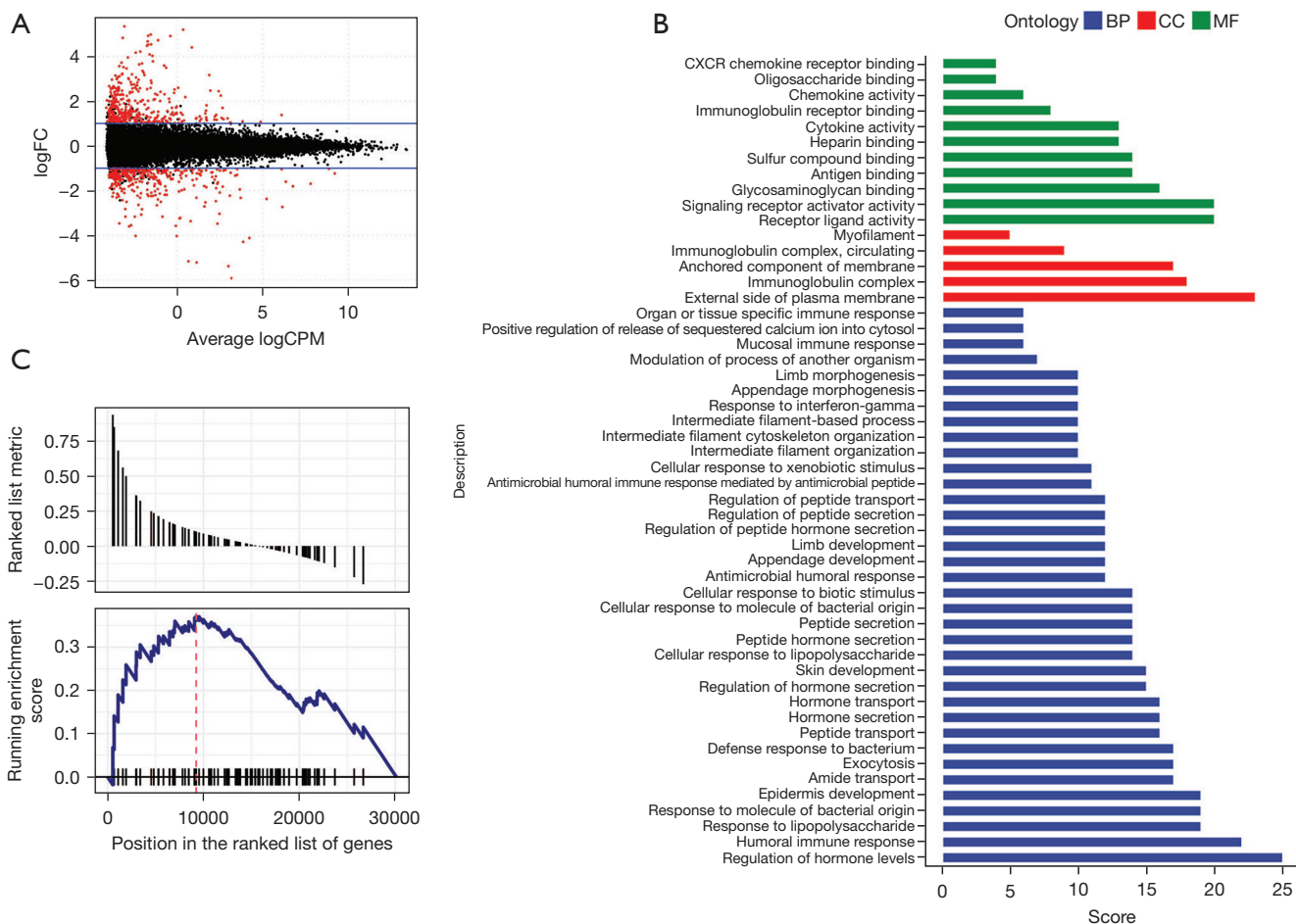


Figure 1 TCGA database analysis results. (A) A total of 318 statistically significant DEGs were identified between high-grade and low-grade CRC groups. Volcano plot showing 225 up-regulated and 93 down-regulated DEGs. Red dots: the genes that differ significantly between high-grade and low-grade CRC groups; black dots: the genes with no significant difference. (B) GO enrichment analysis for DEGs between high- and low-grade CRC groups. Blue, red, and green represent enriched GO terms in the “biological process”, “cellular component”, and “molecular function” categories, respectively. The X-axis and Y-axis represent the count of DEGs and different categories, respectively. (C) Enrichment plot for the STING pathway according to GSEA. TCGA, The Cancer Genome Atlas; FC, fold change; CPM, counts per million; DEGs, differentially expressed genes; CRC, colorectal cancer; GO, Gene Ontology; BP, biological process; CC, cellular component; MF, molecular function; GSEA, gene set enrichment analysis.

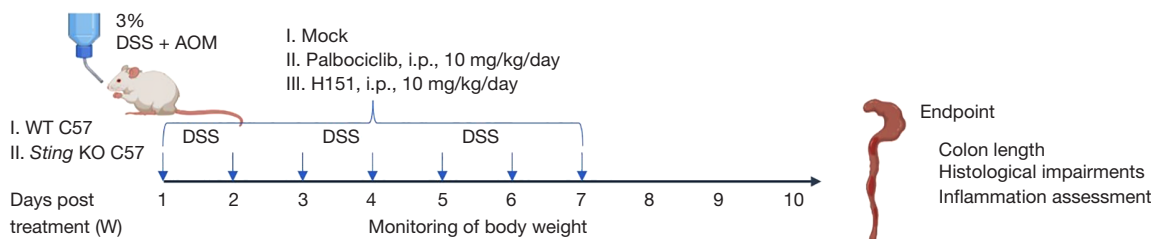


Figure 2 The experimental procedure for the evaluation of the effects of palbociclib and H-151 on DSS/AOM-induced CAC in mice. WT, wild type; DSS, dextran sulfate sodium; AOM, azoxymethane; CAC, colitis-associated colorectal cancer.

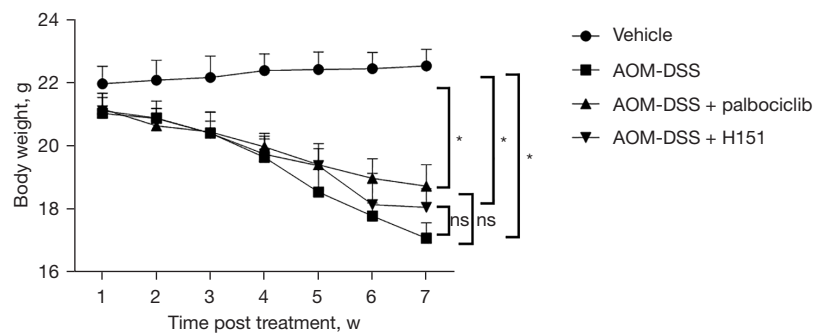


Figure 3 Comparison of body weight of the four groups of mice with different treatments. As compared to the control group, AOM/DSS significantly resulted in significant body weight reduction, which was alleviated following treatment with palbociclib or H-151. *, $P < 0.05$; ns, not significant. AOM, azoxymethane; DSS, dextran sulfate sodium.

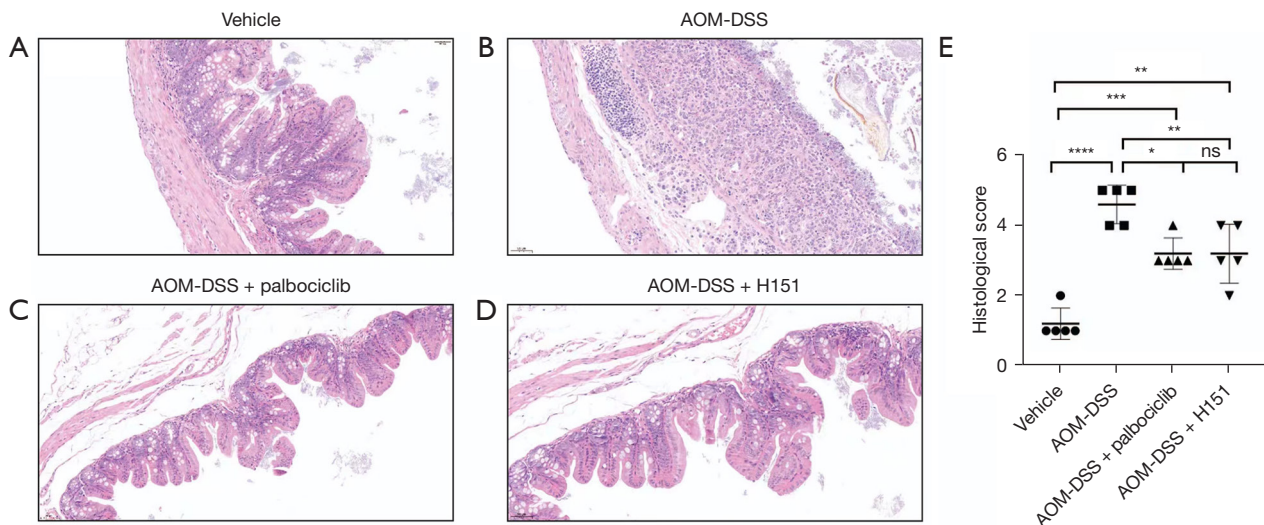


Figure 4 Palbociclib alleviates colon tissue damage in AOM/DSS-induced mice with colon cancer. (A-D) Representative H&E staining of histological changes in the colon tissues of different groups of mice (20 \times). (E) Histological scoring of colonic mucosal damage in different groups of mice. *, $P < 0.05$; **, $P < 0.01$; ***, $P < 0.001$; ****, $P < 0.0001$; ns, not significant. AOM, azoxymethane; DSS, dextran sulfate sodium; H&E, hematoxylin and eosin.

infiltration reduced in these mice (Figure 4C,4D). The histological scores of colon tissue mucosal injury in different groups of mice relative to those of mice in group 2 were assessed. The scores of mice in the drug treatment group (groups 3 and 4) decreased significantly ($P < 0.05$, Figure 4E).

Effects of palbociclib on the levels of *Ifnb1*, *Il6*, and *Il1b* in the colonic mucosa of experimental mice

The transcriptional levels of STING downstream effectors, namely *Ifnb1*, *Il6*, and *Il1b* were measured in the colon tissue. The expression levels of *Ifnb1*, *Il6*, and *Il1b* were

significantly high in the colon tissue of AOM/DSS-induced mice, which was decreased significantly following treatment with palbociclib or H-151 as shown in Figure 5. This suggested the protective role of palbociclib in AOM/DSS-induced inflammation-related CRC. These findings indicated that palbociclib attenuated colorectal inflammation associated with tumorigenesis.

Discussion

CAC is a potentially serious complication of long-term IBD with an estimated incidence of approximately 5% after

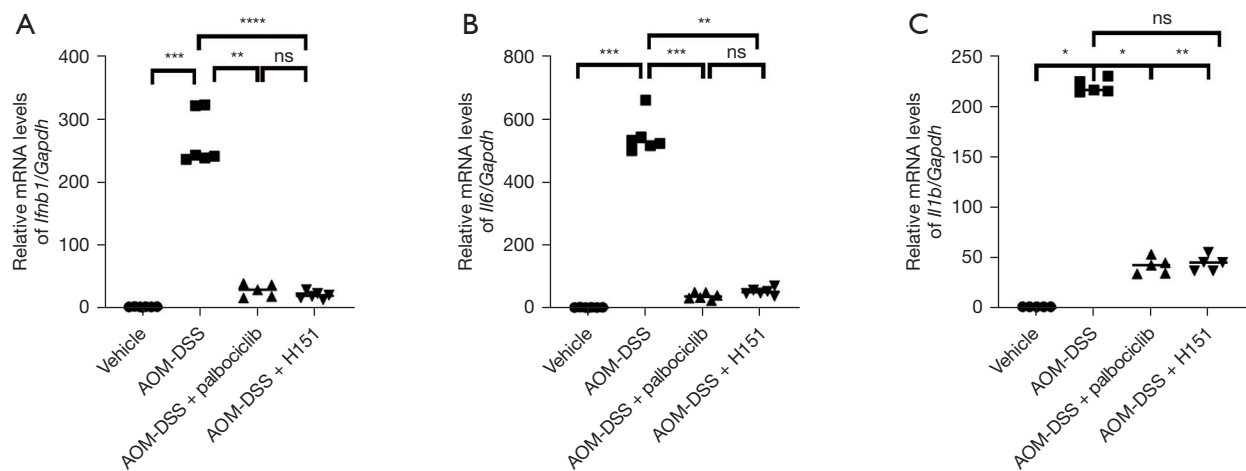


Figure 5 Transcript levels of *Ifnb1*, *Il6*, and *Il1b* in colon tissues of mice in different groups. Following AOM/DSS treatment, the transcription of *Ifnb1* (A), *Il6* (B), and *Il1b* (C) increased significantly in the colon tissues of mice, which was inhibited following palbociclib or H-151 treatment. *, $P < 0.05$; **, $P < 0.01$; ***, $P < 0.001$; ****, $P < 0.0001$; ns, not significant. AOM, azoxymethane; DSS, dextran sulfate sodium.

20 years (13). Patients with IBD show a substantially enhanced risk of developing CRC as compared to those without a history of colitis (14).

Studies have shown that the STING pathway plays an important role in colorectal inflammation and tumorigenesis (5,6,15). In this study, the STING pathway was confirmed to be closely related to CRC based on bioinformatic analysis. Palbociclib was identified as a potent inhibitor of the STING pathway with protective effects against colitis in our previous study (8). We found that palbociclib protects against STING-driven hyperinflammation and pathological damage in *Trex1*^{-/-} mice, providing additional evidence that the *in vivo* effect of palbociclib is STING specific. Herein, we established a CAC mouse model and the protective effects of palbociclib on CAC were confirmed. Recent research has provided evidence that the cGAS-STING pathway plays a crucial role in various anti-tumor treatments. It has been observed that tumor-derived DNA is present in the cytosol of tumor-infiltrating dendritic cells (DCs) and can activate this pathway. This activation leads to the promotion of tumor-specific antigen presentation and activation of cytotoxic T lymphocytes (CTLs) (16,17). Notably, mice lacking the STING protein fail to stimulate CD8⁺ T cells in response to different anti-tumor therapies. Furthermore, another study has demonstrated that activating the STING pathway enhances the anti-tumor responses against both CD8⁺ T cell-sensitive and CD8⁺ T cell-resistant tumors (18). A study showed

that the cGAS/STING signaling pathway is a tumor suppressor of CRC, and the STING cascade constitutes a key component of early host responses to intestinal injury, which are crucial for activating tissue repair pathways to prevent tumorigenesis (19). In addition, a recent study has revealed that *F. nucleatum*, a bacterium associated with CRC, induces the expression of programmed death ligand 1 (PD-L1) by activating the STING signaling pathway. This activation also increases the accumulation of interferon-gamma (IFN- γ)⁺ CD8⁺ tumor-infiltrating lymphocytes (TILs) during PD-L1 blockade treatment, thereby enhancing the tumor's sensitivity to PD-L1 blockade (20). STING agonists, such as DMXAA and 3'3'-cGAMP, can inhibit colon cancer development in mice likely by reducing adenocarcinoma and tumor atypia and increasing immune cell infiltration levels (21).

The presence of the cGAS/STING signaling pathway in macrophages and various immune cells, along with its involvement in regulating and activating senescence, senescence-associated secretory phenotypes (SASPs) secretion, and proinflammatory immune response, implies its potential role in the development of immunosenescence and inflammation (22). A research study demonstrated that the absence of STING signaling hindered the induction of type I interferon in DNA-damaged melanoma cells, while leaving the senescence-related processes unaffected in their model (23).

However, the pathogenesis of CAC is different from that

of sporadic CRC. CAC goes through “inflammation-atypical hyperplasia-cancerization” course, where inflammation serves a crucial role in its progression and occurrence (24). This may be the reason why STING plays different roles in CRC and shows distinct pathogeneses.

In our study, palbociclib and H-151 were selected to treat AOM/DSS-induced inflammation-related CRC in mice. H-151 is a potent, selective, and covalent antagonist of STING both in mice and humans, and is currently the most used compound in the study of autoimmunity and inflammation diseases (25,26). Research shows that H-151 can target Cys91 of STING and block its palmitoylation, thus attenuating STING-mediated tissue damages and IFN β production in Trex1 knockout mice (7). Therefore, H-151 was selected as the control for the role of palbociclib in our study. The results show that both palbociclib and H-151 can play similar roles in alleviating AOM/DSS-induced colonic epithelial damage by inhibiting the transcription of downstream inflammatory factors of the STING pathway. Palbociclib and H-151 alleviate CAC by inhibiting the inflammatory responses of the STING pathway and reducing inflammatory stimulation of the colonic mucosa. Although the body weight of the H-151-treated group and palbociclib-treated group did not reach statistical significance compared with the AOM/DSS group, a trend was still observed. This was probably due to the shorter treatment and observation time, as well as the smaller sample size. Furthermore, pathological examination also showed that palbociclib and H-151 could alleviate the damage of intestinal epithelium after treatment. All the above suggests that palbociclib and H-151 have potential therapeutic value for the treatment of CAC.

Palbociclib, a highly selective reversible CDK4/6 kinase inhibitor, has recently been approved by the United States Food and Drug Administration (FDA) for the treatment of advanced breast cancer (27). Several studies have shown that the combination of palbociclib and other chemotherapy agents or targeted therapies could provide a promising therapeutic alternative for the treatment of CRC. The synergistic effect of palbociclib and a MEK inhibitor has been confirmed in KRAS mutant colon cancer *in vivo* (28-30). Palbociclib (CDK 4/6 inhibitor) and PD0325901 (selective MEK1/2 inhibitor) combinatorial treatment selectively in KRAS-dependent and BRAF-mutant CRC (30). According to the study published by Lee *et al.* (28), the combination of palbociclib and gedatolisib (PI3K/mTOR dual inhibitors) has synergistic anti-proliferative effects in both wild-type

and mutated CRC cell lines and the effect was superior to the combination of palbociclib and PD0325901. The expression of p27kip1 was inversely correlated with palbociclib response, which could be used as a biomarker for palbociclib sensitivity in KRAS mutant CRC (31). Research has shown that palbociclib could synergistically cooperate with irinotecan against CRC under hypoxic conditions by deregulating the phosphorylation of CDK6 and Rb induced by irinotecan (32). The combination of ERK1/2 inhibitor SCH772984 and palbociclib has shown significant inhibition of tumor growth of CRC *in vivo* (33). A clinical trial confirmed the safety and efficacy of the combinatory treatment using both binimetinib and palbociclib in metastatic CRC patients carrying RAS mutations, which was evaluated using patient-derived xenografts (PDX) (34). In addition, there were reports that palbociclib could be a novel radiosensitizer agent (35,36). A study showed that the existence of p53 wild type was required for the radiosensitizing effect of palbociclib, which had nothing to do with the inhibition of CDK4/6 (37). Furthermore, some biomarkers have the potential to be used for diagnosis and predicting treatment outcomes of CRC (31,38).

Our previous work showed that palbociclib inhibited the STING inflammatory pathway independently of the CDK pathway. In DSS-induced mice colon tissue, the abundance of downstream effectors of STING, as evidenced by the enhanced transcripts of *Ifnb1*, *Il6*, and *Il1b*, suggested transcriptional upregulation. Whereas treatment with palbociclib or H-151 almost abolished this response (8). The transcription of *Ifnb1*, *Il6*, and *Il1b* was upregulated in the colon of mice with AOM/DSS-induced inflammation-associated CRC, which was inhibited after treatment with palbociclib or H-151. This observation suggested a potential link between the impact of palbociclib on inflammation-related CRC and the modulation of the STING pathway. Taken together, by inhibiting inflammatory responses, palbociclib may exert protective effects on CAC. Palbociclib is a marketed drug that has been used in the treatment of breast cancer. Our study provides the basis for the use of this FDA-approved drug in the treatment of CAC. In addition, these findings provide valuable insights and warrant further comprehensive mechanistic studies in this area.

This study also has several limitations: first, the TCGA database cases cannot be further selected for CAC. Second, further research and validation of clinical samples are needed to clarify the role of palbociclib in CAC. In the

future, more in-depth mechanism research will be needed to discover the key factors on which palbociclib acts in CAC, as well as the biological markers.

Conclusions

In conclusion, palbociclib, a STING antagonist, suppressed colon carcinogenesis likely through the attenuation of the inflammation pathway of the colon. More studies are needed to identify the mechanisms underlying palbociclib's protective effect.

Acknowledgments

Funding: This study was supported by the National Natural Science Foundation of China (No. 82002416 to L.Y.).

Footnote

Reporting Checklist: The authors have completed the ARRIVE reporting checklist. Available at <https://jgo.amegroups.com/article/view/10.21037/jgo-23-860/rc>

Data Sharing Statement: Available at <https://jgo.amegroups.com/article/view/10.21037/jgo-23-860/dss>

Peer Review File: Available at <https://jgo.amegroups.com/article/view/10.21037/jgo-23-860/prf>

Conflicts of Interest: All authors have completed the ICMJE uniform disclosure form (available at <https://jgo.amegroups.com/article/view/10.21037/jgo-23-860/coif>). L.Y. reports funding support from the National Natural Science Foundation of China (grant number: 82002416). The other authors have no conflicts of interest to declare.

Ethical Statement: The authors are accountable for all aspects of the work in ensuring that questions related to the accuracy or integrity of any part of the work are appropriately investigated and resolved. The study was conducted in accordance with the Declaration of Helsinki (as revised in 2013). All animal experiments were performed under a project license (No. K23-048Y) granted by the Ethics Committees of Shanghai Pulmonary Hospital, in compliance with the institutional guidelines for the care and use of animals.

Open Access Statement: This is an Open Access article

distributed in accordance with the Creative Commons Attribution-NonCommercial-NoDerivs 4.0 International License (CC BY-NC-ND 4.0), which permits the non-commercial replication and distribution of the article with the strict proviso that no changes or edits are made and the original work is properly cited (including links to both the formal publication through the relevant DOI and the license). See: <https://creativecommons.org/licenses/by-nc-nd/4.0/>.

References

1. Sung H, Ferlay J, Siegel RL, et al. Global Cancer Statistics 2020: GLOBOCAN Estimates of Incidence and Mortality Worldwide for 36 Cancers in 185 Countries. *CA Cancer J Clin* 2021;71:209-49.
2. Beaugerie L, Itzkowitz SH. Cancers complicating inflammatory bowel disease. *N Engl J Med* 2015;372:1441-52.
3. Watanabe T, Konishi T, Kishimoto J, et al. Ulcerative colitis-associated colorectal cancer shows a poorer survival than sporadic colorectal cancer: a nationwide Japanese study. *Inflamm Bowel Dis* 2011;17:802-8.
4. Yaeger R, Shah MA, Miller VA, et al. Genomic Alterations Observed in Colitis-Associated Cancers Are Distinct From Those Found in Sporadic Colorectal Cancers and Vary by Type of Inflammatory Bowel Disease. *Gastroenterology* 2016;151:278-287.e6.
5. Ma C, Yang D, Wang B, et al. Gasdermin D in macrophages restrains colitis by controlling cGAS-mediated inflammation. *Sci Adv* 2020;6:eaaz6717.
6. Ahn J, Son S, Oliveira SC, et al. STING-Dependent Signaling Underlies IL-10 Controlled Inflammatory Colitis. *Cell Rep* 2017;21:3873-84.
7. Haag SM, Gulen MF, Reymond L, et al. Targeting STING with covalent small-molecule inhibitors. *Nature* 2018;559:269-73.
8. Gao J, Zheng M, Wu X, et al. CDK inhibitor Palbociclib targets STING to alleviate autoinflammation. *EMBO Rep* 2022;23:e53932.
9. Wang L, Tang L, Feng Y, et al. A purified membrane protein from *Akkermansia muciniphila* or the pasteurised bacterium blunts colitis associated tumourigenesis by modulation of CD8(+) T cells in mice. *Gut* 2020;69:1988-97.
10. Ibrahim A, Hugerth LW, Hases L, et al. Colitis-induced colorectal cancer and intestinal epithelial estrogen receptor beta impact gut microbiota diversity. *Int J Cancer* 2019;144:3086-98.

11. Wu N, Feng YQ, Lyu N, et al. *Fusobacterium nucleatum* promotes colon cancer progression by changing the mucosal microbiota and colon transcriptome in a mouse model. *World J Gastroenterol* 2022;28:1981-95.
12. Livak KJ, Schmittgen TD. Analysis of relative gene expression data using real-time quantitative PCR and the 2(-Delta Delta C(T)) Method. *Methods* 2001;25:402-8.
13. Dulai PS, Sandborn WJ, Gupta S. Colorectal Cancer and Dysplasia in Inflammatory Bowel Disease: A Review of Disease Epidemiology, Pathophysiology, and Management. *Cancer Prev Res (Phila)* 2016;9:887-94.
14. Baker AM, Cross W, Curtius K, et al. Evolutionary history of human colitis-associated colorectal cancer. *Gut* 2019;68:985-95.
15. Martin GR, Blomquist CM, Henare KL, et al. Stimulator of interferon genes (STING) activation exacerbates experimental colitis in mice. *Sci Rep* 2019;9:14281.
16. Chen Q, Sun L, Chen ZJ. Regulation and function of the cGAS-STING pathway of cytosolic DNA sensing. *Nat Immunol* 2016;17:1142-9.
17. Wang H, Hu S, Chen X, et al. cGAS is essential for the antitumor effect of immune checkpoint blockade. *Proc Natl Acad Sci U S A* 2017;114:1637-42.
18. Nicolai CJ, Wolf N, Chang IC, et al. NK cells mediate clearance of CD8(+) T cell-resistant tumors in response to STING agonists. *Sci Immunol* 2020;5:eaaz2738.
19. Ahn J, Konno H, Barber GN. Diverse roles of STING-dependent signaling on the development of cancer. *Oncogene* 2015;34:5302-8.
20. Gao Y, Bi D, Xie R, et al. *Fusobacterium nucleatum* enhances the efficacy of PD-L1 blockade in colorectal cancer. *Signal Transduct Target Ther* 2021;6:398.
21. Gong W, Liu P, Zhao F, et al. STING-mediated Syk Signaling Attenuates Tumorigenesis of Colitis-associated Colorectal Cancer Through Enhancing Intestinal Epithelium Pyroptosis. *Inflamm Bowel Dis* 2022;28:572-85.
22. Andrade B, Jara-Gutiérrez C, Paz-Araos M, et al. The Relationship between Reactive Oxygen Species and the cGAS/STING Signaling Pathway in the Inflammaging Process. *Int J Mol Sci* 2022;23:15182.
23. Chavanet A, Hill KR, Jiménez-Andrade Y, et al. Intracellular signaling modules linking DNA damage to secretome changes in senescent melanoma cells. *Melanoma Res* 2020;30:336-47.
24. Biancone L, Armuzzi A, Scribano ML, et al. Cancer Risk in Inflammatory Bowel Disease: A 6-Year Prospective Multicenter Nested Case-Control IG-IBD Study. *Inflamm Bowel Dis* 2020;26:450-9.
25. Liu C, Tang J, Luo W, et al. DNA from macrophages induces fibrosis and vasculopathy through POLR3A/STING/type I interferon axis in systemic sclerosis. *Rheumatology (Oxford)* 2023;62:934-45.
26. Pan Y, You Y, Sun L, et al. The STING antagonist H-151 ameliorates psoriasis via suppression of STING/NF-κB-mediated inflammation. *Br J Pharmacol* 2021;178:4907-22.
27. Finn RS, Crown JP, Lang I, et al. The cyclin-dependent kinase 4/6 inhibitor palbociclib in combination with letrozole versus letrozole alone as first-line treatment of oestrogen receptor-positive, HER2-negative, advanced breast cancer (PALOMA-1/TRIO-18): a randomised phase 2 study. *Lancet Oncol* 2015;16:25-35.
28. Lee CL, Cremona M, Farrelly A, et al. Preclinical evaluation of the CDK4/6 inhibitor palbociclib in combination with a PI3K or MEK inhibitor in colorectal cancer. *Cancer Biol Ther* 2023;24:2223388.
29. Ziemke EK, Dosch JS, Maust JD, et al. Sensitivity of KRAS-Mutant Colorectal Cancers to Combination Therapy That Cotargets MEK and CDK4/6. *Clin Cancer Res* 2016;22:405-14.
30. Pek M, Yatim SMJM, Chen Y, et al. Oncogenic KRAS-associated gene signature defines co-targeting of CDK4/6 and MEK as a viable therapeutic strategy in colorectal cancer. *Oncogene* 2017;36:4975-86.
31. Rampioni Vinciguerra GL, Dall'Acqua A, Segatto I, et al. p27kip1 expression and phosphorylation dictate Palbociclib sensitivity in KRAS-mutated colorectal cancer. *Cell Death Dis* 2021;12:951.
32. Zhang J, Zhou L, Zhao S, et al. The CDK4/6 inhibitor palbociclib synergizes with irinotecan to promote colorectal cancer cell death under hypoxia. *Cell Cycle* 2017;16:1193-200.
33. Zhang Y, Wang D, Lv B, et al. Oleic Acid and Insulin as Key Characteristics of T2D Promote Colorectal Cancer Deterioration in Xenograft Mice Revealed by Functional Metabolomics. *Front Oncol* 2021;11:685059.
34. Sorokin AV, Kanikarla Marie P, Bitner L, et al. Targeting RAS Mutant Colorectal Cancer with Dual Inhibition of MEK and CDK4/6. *Cancer Res* 2022;82:3335-44.
35. Tao Z, Le Blanc JM, Wang C, et al. Coadministration of Trametinib and Palbociclib Radiosensitizes KRAS-Mutant Non-Small Cell Lung Cancers In Vitro and In Vivo. *Clin Cancer Res* 2016;22:122-33.
36. Whittaker S, Madani D, Joshi S, et al. Combination of

- palbociclib and radiotherapy for glioblastoma. *Cell Death Discov* 2017;3:17033.
37. Fernández-Aroca DM, Roche O, Sabater S, et al. P53 pathway is a major determinant in the radiosensitizing effect of Palbociclib: Implication in cancer therapy. *Cancer Lett* 2019;451:23-33.
38. Dai W, Wang Z, Liang X, et al. Circulating lncRNA EGFR-AS1 as a diagnostic biomarker of colorectal cancer and an indicator of tumor burden. *J Gastrointest Oncol* 2022;13:2439-46.

Cite this article as: Yang L, Gao J, Zhang Y, Perez EA, Wu Y, Guo T, Li C, Wang H, Xu Y. Protective effects of palbociclib on colitis-associated colorectal cancer. *J Gastrointest Oncol* 2023;14(6):2436-2447. doi: 10.21037/jgo-23-860